ELSEVIER

Biophysical Chemistry 72 (1998) 297–306

Biophysical Chemistry

Effect of base composition on DNA bending by phosphate neutralization

Juliane K. Strauss-Soukup [a,b,1], Paula D. Rodrigues [b], L. James Maher III [b,*]

[a] *Department of Biochemistry and Molecular Biology and Eppley Institute for Research in Cancer and Allied Diseases, University of Nebraska Medical Center, Omaha, NE 68198, USA*

[b] *Department of Biochemistry and Molecular Biology, Mayo Foundation, Rochester, MN 55905, USA*

Received 15 October 1997; revised 9 February 1998; accepted 9 February 1998

Abstract

Of the many forces involved in DNA bending by proteins, we have focused on the possible role of asymmetric phosphate neutralization due to interactions between the negatively charged phosphate backbone of duplex DNA and cationic amino acids of an approaching protein. The resulting unbalanced charge distribution along the duplex DNA is thought to induce the double helix to collapse toward the neutralized surface. Previous work has confirmed that DNA bending ($\sim 20.7 \pm 4°$) is induced by asymmetric incorporation of six uncharged racemic methylphosphonate analogs partially neutralizing one face of GC-rich duplex DNA. We have now analyzed DNA duplexes with similar patches of methylphosphonate linkages in an AT-rich sequence context and again observe bending toward the neutralized face, to an extent ($20 \pm 0.6°$) comparable to that observed for neutral patches in GC-rich DNA. The similar induced bend angles in AT-rich and GC-rich contexts does not reveal increased flexibility in AT-rich sequences, or a particular propensity of A–T base pairs to roll toward the minor groove in the tested sequences.

Keywords: DNA bending; Methylphosphonate; Phosphate neutralization; Electrostatic; A tract; Electrophoresis

1. Introduction

Asymmetric neutralization of the phosphate backbone of duplex DNA by cationic amino acids has been suggested as a driving force in DNA bending by proteins such as histones [1,2]. According to this view, phosphate neutralization on one face of the double helix induces an unbalanced charge distribution along the DNA. The double helix is then envisioned to collapse toward the neutralized surface in response to asymmetric electrostatic repulsions. Experimental evidence tends to support this hypothesis. For example, asymmetric incorporation of six racemic methylphosphonate linkages to create a neutralized region on one face of duplex DNA induced $\sim 20°$ of bending [3]. In these previous experiments, neutralization involved modifications arranged across one minor groove of DNA in a GC-rich sequence context. It is of interest to know how base-pair (bp)

* Corresponding author.

[1] Present address: Department of Molecular Biophysics, Yale University, PO Box 20814, 260 Whitney Ave., New Haven, CT, 06520-8114.

0301-4622/98/$19.00
PII S0301-4622(98)00112-4

composition influences DNA bending by phosphate neutralization.

In this study, we compare the direction and magnitude of DNA bending by phosphate neutralization in an AT-rich sequence context. Binding sites for many DNA bending proteins are AT-rich [4–10]. Theoretical studies suggest that G–C vs. A–T bp differ in their intrinsic propensities to induce DNA curvature by roll toward the major vs. minor grooves [11,12]. We hypothesized that neutralized phosphates arrayed across the minor groove of an AT-rich sequence would induce a greater DNA bend than in a GC-rich context due to the inherent tendency of AT-rich sequences to roll toward the minor groove. The results of the present study do not confirm this prediction; DNA bending induced in the AT-rich sequence was comparable to that previously observed in GC-rich DNA.

2. Materials and methods

2.1. Oligonucleotides

Unmodified oligonucleotides were prepared using an abi model 394 dna synthesizer according to standard procedures. Oligonucleotides were cleaved from the synthesis column and deprotected in hot ammonia. Oligonucleotides containing site-specific racemic methylphosphonate substitutions were synthesized at 1 μmol scale using methylphosphonamidite monomers obtained from Glen Research (Sterling, VA). Isobutyryl derivatives of cytosine were used to facilitate cleavage from the solid support and deprotection as previously described [13]. All oligomers were purified by denaturing polyacrylamide gel electrophoresis, eluted from the gel, and desalted using c18 reverse phase cartridges. Oligonucleotide concentrations were determined at 260 nm using molar extinction coefficients (m^{-1} cm^{-1}) of 15,400 (A), 11,700 (G), 7300 (C), 8800 (T) assuming no hypochromicity.

2.2. Detection of DNA shape by gel electrophoresis

Analysis of DNA shape was performed by comparative gel electrophoresis of ligated DNA duplexes as previously described [3,14]. Relative curvature values and estimates of electrostatic bend angles were determined as previously described [3,14,15]. Briefly, the distance migrated by duplex DNA standards of known length was measured and fit by a least-squares method to an exponential function. The apparent length of ligated DNA in each gel band was then estimated using the derived function and the distance migrated. An equation of the form:

$$R_L - 1 = \left(pL^2 - q \right)(\text{relative curvature})^2$$

where R_L is the ratio of apparent DNA length to actual DNA length, and L is the actual DNA length, was fit by a least-squares method to data for duplexes containing one A_6 tract per 21 bp (relative curvature = 0.5 A_6 tract equivalents per helical turn) and no neutral phosphates. Estimates for the values of the constants, p and q, were determined for each gel. The resulting equation was then used to obtain estimates for unknown relative curvature values for duplexes containing both an A_6 tract and neutralized phosphates. Estimates for the magnitude of the electrostatic bend, b, were calculated by obtaining the least-squares fit of the phasing equation:

$$c = \left[a^2 + b^2 - 2ab\cos(180 - \theta) \right]^{0.5}$$

to plots of the net curvature vs. radial angle between neutral patch and A_6 tract, θ. Constant a is the magnitude of the curvature due to the A_6 tract (0.5 A_6 tract equivalents per helical turn). Dependent variable c is the measured value of the net curvature (same units), and b is the unknown magnitude of the electrostatic bend (same units). Estimates of the electrostatic bend in degrees were obtained using a value of 18° for the deflection of the DNA helix axis by a single A_6 tract in duplex **7** [14].

2.3. Thermal melting of oligonucleotide duplexes

Pairs of oligonucleotides were diluted to 5×10^{-7} M in 0.05 M MOPS pH 7.1 in a final volume of 1 ml. Thermal melting studies were then performed in reduced-volume Hellma quartz 114B-QS self-masking cuvettes of 1 cm path length. Data were collected using a Cary 3 UV spectrophotometer. The temperature was controlled and monitored by a Peltier temperature controller (Varian), from a starting temperature of 5°C to a final temperature of 95°C, at a rate

of 0.5°C per min. The sample compartment was flushed with nitrogen during the low temperature portion of the analysis to prevent condensation of atmospheric moisture on the cuvettes. An averaged absorbance was determined every 12 s for each cell. Data were exported to the data analysis program Kaleidagraph™ (Synergy Software), and the melting transition temperature (T_m, °C) was determined as the maximum of a plot of the first derivative of absorbance vs. temperature.

3. Results and discussion

3.1. Approach

Native gel electrophoresis has been used to study intrinsic and induced DNA bending [3,14,15]. The mobility of DNA fragments through native polyacrylamide gels exhibits remarkable shape dependence. For DNA molecules of identical mass, curvature results in decreased mobility. In the present study, DNA duplexes forming two turns of the double helix are ligated into polymers. DNA shape is then analyzed using the phasing method [14]. Phasing analysis is a sensitive and powerful approach because it permits estimation of both the magnitude and direction of an induced bend. An uncharacterized site of helix deformation (in this case, a bend induced by electrostatic effects) is placed at different spacings relative to an internal reference deformation (an A_6 tract whose magnitude and direction are well characterized [14]. Molecules wherein the reference deformation is enhanced by proper phasing with an electrostatic bend exhibit reduced electrophoretic mobility relative to other phasings. Because all molecules are composed of duplexes of identical molecular weight and charge, mobility differences can be attributed entirely to molecular shape.

3.2. Determination of helical repeat parameters for synthetic duplexes

Phasing analysis requires confirmation of the helical repeat parameter (number of bp per helical turn of DNA) for each group of test sequences. To measure the helical repeat of DNAs modified with methylphosphonate linkages, we monitored gel mobility as a function of duplex length for duplexes having A_6 tract curvature and methylphosphonate substitutions on the same face (*cis* configuration). Duplex length was varied from 20 to 22 bp. Synthetic duplexes **1–3** were synthesized for this purpose (Fig. 1). The helical repeat was determined by finding the duplex length that produced the greatest electrophoretic anomaly, corresponding to the arrangement wherein elements of curvature are phased most exactly with each other (Fig. 2, compare lanes 7, 10, and 12). Analysis of the dependence of gel mobility

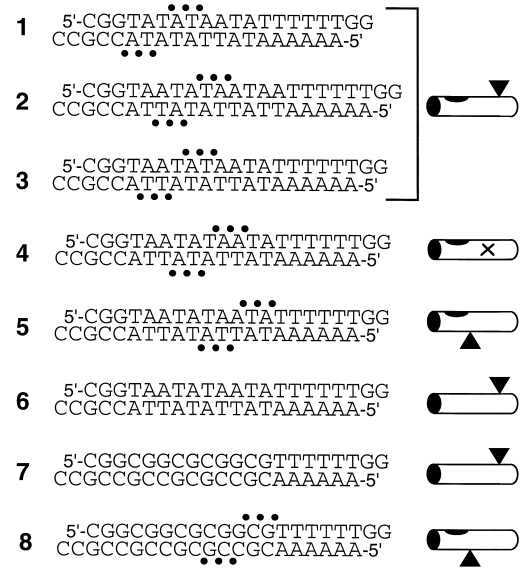

Fig. 1. Synthetic oligonucleotides for helical repeat and phasing experiments. Duplexes **1–3** (20 bp, 22 bp, and 21 bp in length, respectively) were used to establish the helical repeat of DNA containing neutral methylphosphonate linkages. Sites of racemic methylphosphonate substitution are identified (●). Cylinders at right depict elements of curvature. The direction of intrinsic curvature due to an A_6 tract results in the right end of the double helix curving upward at the filled arrowhead. When oriented into the page, the filled arrowhead is shown as an 'X'. The filled oval depicts the helical face neutralized by methylphosphonate substitutions. Duplexes **3**, **4**, and **5** are 21 bp in length and contain the neutralized sequence in different phasings relative to the stationary A_6 tract. In duplex **3**, the minor groove at the center of the neutralized sequence is on the same helical face as the bend due to the A_6 tract (elements separated by ~49°; *cis* configuration). In duplex **4**, these elements are separated by ~118° (orthogonal configuration). In duplex **5**, the separation is ~189° (*trans* configuration). Duplex **6** is an unmodified standard that contains a single A_6 tract in an AT-rich sequence context, whereas the context is GC-rich in duplex **7**.

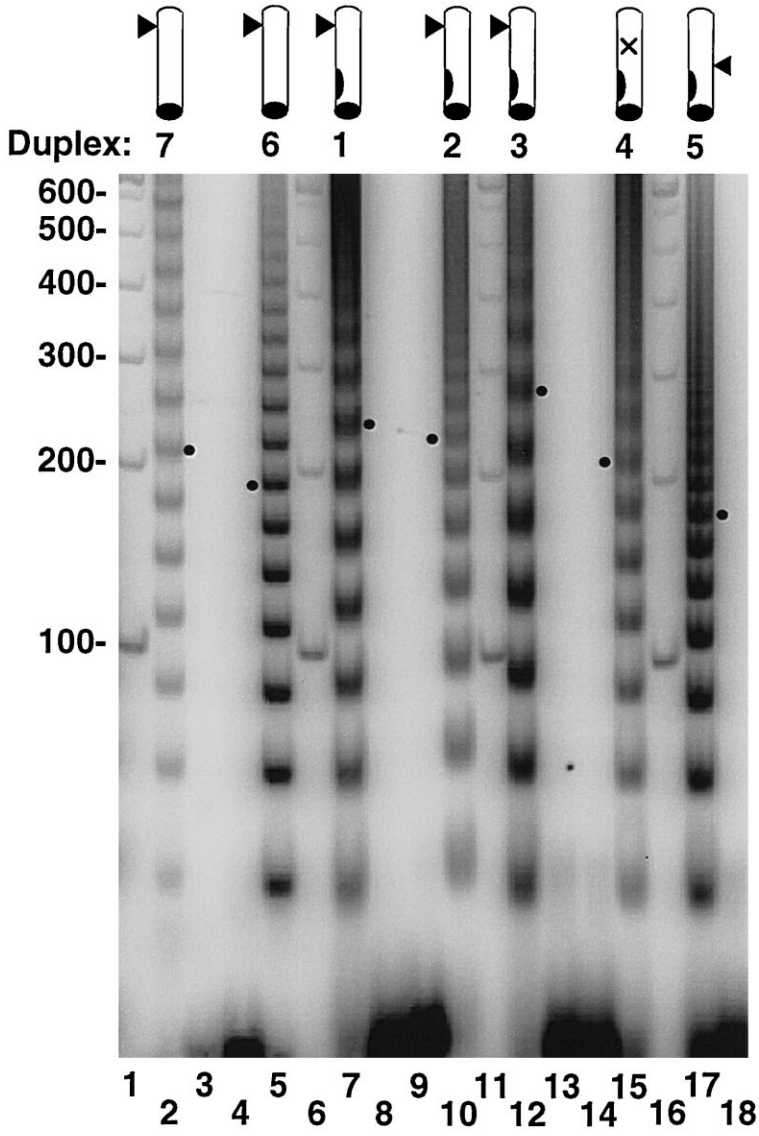

Fig. 2. Electrophoretic assay of DNA shape. Labeled DNA duplexes were ligated and analyzed by electrophoresis through nondenaturing polyacrylamide gels as described in Section 2. Duplex DNA ladders, 100 bp, (lengths indicated at left) are included for reference (lanes 1, 6, 11, and 16). Samples without DNA ligase (lanes 3, 4, 8, 9, 13, 14, and 18) contain only 21 bp species. The 168 bp species (●) is indicated for each ligated sample.

anomaly (R_L) on duplex length shows that the helical repeat of duplexes containing methylphosphonate linkages is 10.4 ± 0.01 bp per helical turn, near the canonical value for B-DNA (Fig. 3). The helical repeat of unmodified duplexes was also determined (data not shown) and was found to be 10.5 ± 0.01 bp per helical turn. Subsequent experiments to study the behavior of two helical turns of modified DNA therefore employed 21-bp duplexes.

3.3. Duplexes with methylphosphonate linkages in an AT-rich sequence context

We monitored DNA bending induced by site specific neutralization of duplex DNA with methylphos-

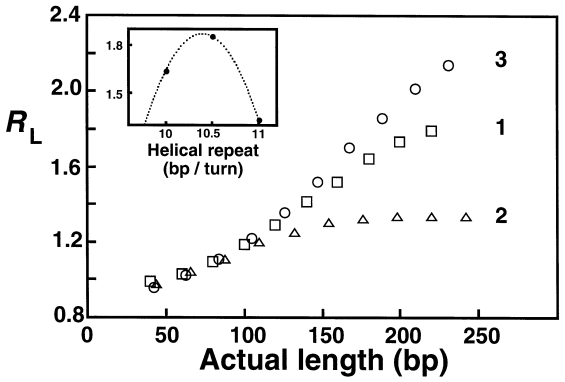

Fig. 3. Experimental measurement of DNA helical repeat. Mobilities are shown for ligated duplexes **1** (□), **2** (△) and **3** (○) containing the *cis* configuration of methylphosphonate linkages relative to an A_6 tract in duplexes of lengths 20 bp, 22 bp and 21 bp, respectively. The inset depicts R_L values for the 189 bp species (average from two experiments) as a function of helical repeat. The overall helical repeat parameter (10.4 bp/helical turn) was estimated as the value of the *x*-axis at the maximum of a parabolic function fit to the data (inset: dotted curve). SD of the R_L estimates were less than 0.01.

phonate linkages arrayed across the minor groove on one face of the double helix (Fig. 1). Duplex **3** contains the *cis* phasing arrangement (the center of curvature due to the reference A_6 tract lies ~49° from the helical face defined by the patch of methylphosphonate linkages). Duplex **4** contains the orthogonal phasing arrangement (centers of curvature of these elements are positioned ~118° away from each other), and duplex **5** contains the *trans* phasing arrangement (centers of curvature are separated by ~189°). Duplex **6** is an unmodified standard that contains a single A_6 tract in an AT-rich sequence context, and duplex **7** is a similar unmodified standard whose A_6 tract has been placed in a GC-rich sequence context. The electrophoretic properties of duplex **7** have been previously studied [3,16]. The curvature of the A_6 tract in duplex **7** is taken to be 18° toward the minor groove in these experiments [14].

Electrophoretic data were obtained to characterize AT-rich duplexes and curvature induced by a patch of six methylphosphonate linkages (Fig. 2). The mobilities of the respective 8-mer ligated products (168 bp actual length) are indicated by dots in Fig. 2. Of immediate note is the fact that unmodified A_6 tract standard duplexes **6** (AT-rich base composition flanking the A_6 tract) and **7** (GC-rich base composition flanking the A_6 tract) do not comigrate (Fig. 2, compare lanes 2 and 5). This result emphasizes that overall DNA curvature induced by an A_6 tract can be modified by the local DNA base composition [17]. In the present case, the AT-rich flanking sequences slightly reduce the apparent bending due to the A_6 tract from 18° to ~13°.

The shapes of partially-neutralized DNA duplexes depends on helical phasing as is evident from the differences in migration of the indicated 8-mer

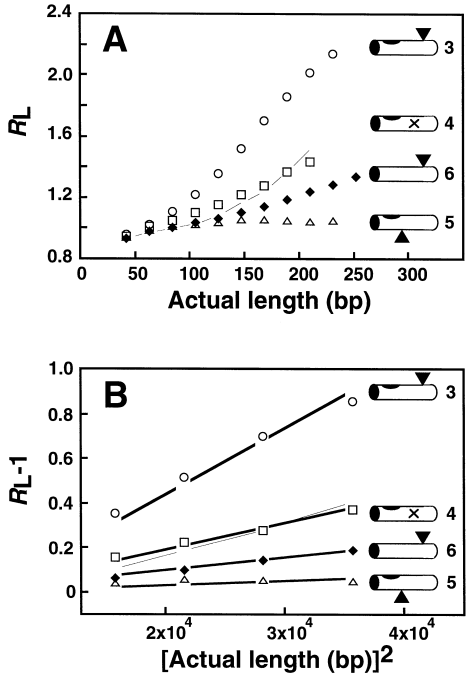

Fig. 4. (A) Graphical depiction of DNA bending induced by incorporation of six methylphosphonate linkages (duplexes **3**, **4** and **5**). Duplex **6** is an unmodified standard that contains a single A_6 tract in an AT-rich sequence context. Apparent lengths of ligated DNA duplexes were calculated relative to a standard curve based on mobilities of the 100-bp duplex DNA ladder. The ratio of apparent length to actual length, (R_L), is plotted vs. actual length for each duplex. Data for GC-rich duplex **7** in the same assay are depicted by a thin line. (B) Estimation of relative DNA curvature (number of A_6 tract equivalents per helical turn). Relative DNA curvature estimates were obtained by fitting data from panel A as described in Section 2, using the behavior of GC-rich duplex **7** (thin line) as a reference. The relative curvature of duplex **7** was set at 0.5 A_6 tract equivalents per helical turn. All relative curvature estimates reflect data from at least three experiments.

species in *cis*, orthogonal and *trans* arrangements (Fig. 2, compare dots beside lanes 12, 15, and 17). The *cis* arrangement of the A_6 tract and neutralized patch results in the slowest rate of migration (Fig. 2, lane 12) suggesting that the curvature due to the patch of methylphosphonate linkages tends to enhance the A_6 tract curvature when the elements are on the same DNA face. This result is in accord with previous studies wherein bending toward the minor groove was observed after phosphate neutralization along the minor groove in a GC-rich sequence context [3]. The ratio of apparent length to actual length (R_L) is plotted vs. the actual length of the duplexes in Fig. 4A. The presence of phased elements of static curvature is manifested by increasingly positive deviations from $R_L = 1.0$ for increasing molecular lengths. Overall, the data in Fig. 4A confirm that the patch of methylphosphonate linkages induces bending toward the minor groove, enhancing the A_6 tract bend. Lowest overall curvature (greatest mobility) is observed for the *trans* phasing.

The mobility data for duplexes containing a patch of methylphosphonate linkages were transformed to allow fitting to linear functions relating gel anomaly to the relative curvature for each phasing (Fig. 4B). Resulting estimates for relative curvature (A_6 tract equivalents per helical turn) were determined for duplexes **3–6** (Table 1), as described in Section 2, using duplex **7** as a standard. Data from all three phasing arrangements were then combined to generate quantitative estimates for induced DNA bending [3]. Relative curvature estimates are plotted as a function of the radial angle between the center of the A_6 tract and the center of the patch of methylphosphonate linkages (Fig. 5). Based on this analysis, the magnitude of the A_6 tract bend in the AT-rich sequence context was taken to be 0.37 A_6 tract equivalents per helical turn, corresponding to 13.2° of DNA curvature. Data fitting to the phasing equation indicates that the magnitude of the bend angle due to the patch of methylphosphonate linkages in an AT-rich sequence context is 20 ± 0.1° toward the

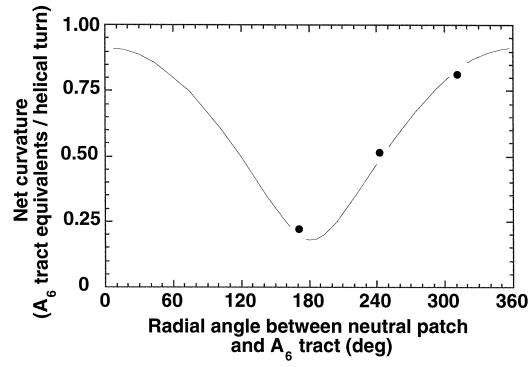

Fig. 5. The interpretation of phasing data for duplexes with methylphosphonate linkages. Plot depicts estimates of the magnitude of net DNA curvature (■) as a function of the radial angle between the A_6 tract and the locus of bending under study. Curve indicates least squares fitting of the phasing data to an empirical cosine function that deconvolutes the net curvature into components due to the A_6 tract and the bending locus under study (see Section 2).

Table 1
DNA bending induced by six neutralized phosphates

21-bp Duplex six neutralizations	Relative curvature[a]		DNA bend angle[b] (°)
GC-rich[c]	unmodified	0.5	18
	cis	0.93 ± 0.01	20.7 ± 4.0
	ortho	0.61 ± 0.02	20.7 ± 4.0
	trans	0.26 ± 0.02	20.7 ± 4.0
AT-rich	unmodified	0.37 ± 0.02	13.2 ± 1.0
	cis	0.81 ± 0.01	20.0 ± 0.1
	ortho	0.52 ± 0.01	20.0 ± 0.1
	trans	0.22 ± 0.01	20.0 ± 0.1

[a]Average ± standard deviation (SD) based on at least three experiments, where 0.5 is the relative curvature due to the A_6 tract present in 21-bp duplex **7**.
[b]Based on best fits to phasing equations. In all cases the indicated bending is toward the minor groove. The average value is given ± SD based on at least three experiments.
[c]Strauss and Maher [3].

minor groove (Table 1). This result is comparable to the previous observation that a patch of six methylphosphonate linkages induces a $20.7 \pm 4°$ DNA bend toward the minor groove in a GC-rich sequence context [3]. The similarity of DNA bending in both AT- and GC-rich sequence contexts does not support our initial hypothesis that equal electrostatic effects would cause unequal DNA bending as a function of base composition.

3.4. Methylphosphonate substitution effects

Our data suggest that the sequence context in which phosphates are neutralized by methylphosphonate substitutions does not dramatically affect induced DNA bending. Implicit in this interpretation are several important assumptions. First, this conclusion has been derived from the study of two DNA sequences that are assumed to be representative. Second, we assume that the similarity in the pattern of phosphate neutralization between this and previous studies [3] causes a comparable electrostatic bending force that is sequence-independent. Third, we assume that any structural perturbations due to the methylphosphonate analogs per se are relatively small and sequence-independent. This view is supported by the results of two previous studies. First, the degree of DNA bending observed after methylphosphonate substitution responds to the presence of multivalent cations as predicted for a structural change induced by an electrostatic effect [3]. Second, we have previously studied DNA bending after substitution using only the structurally-preferred R_P methylphosphonate stereoisomer [18], a strategy designed to minimize helix distortions. These studies showed that steric perturbations attributable to unfavorable methylphosphonate stereoisomers enhance bending by no more than $\sim 30\%$.

To further demonstrate that methylphosphonate substitutions do not greatly perturb DNA duplex structure, we wished to measure the thermal stabilities of the DNA duplexes investigated in this study. We therefore performed thermal denaturation experiments to compare the stabilities of unmodified and modified DNA oligonucleotides. Representative data for AT-rich and GC-rich duplexes are shown in Fig. 6 and Table 2. These results demonstrate that the presence of six racemic methylphosphonate substitu-

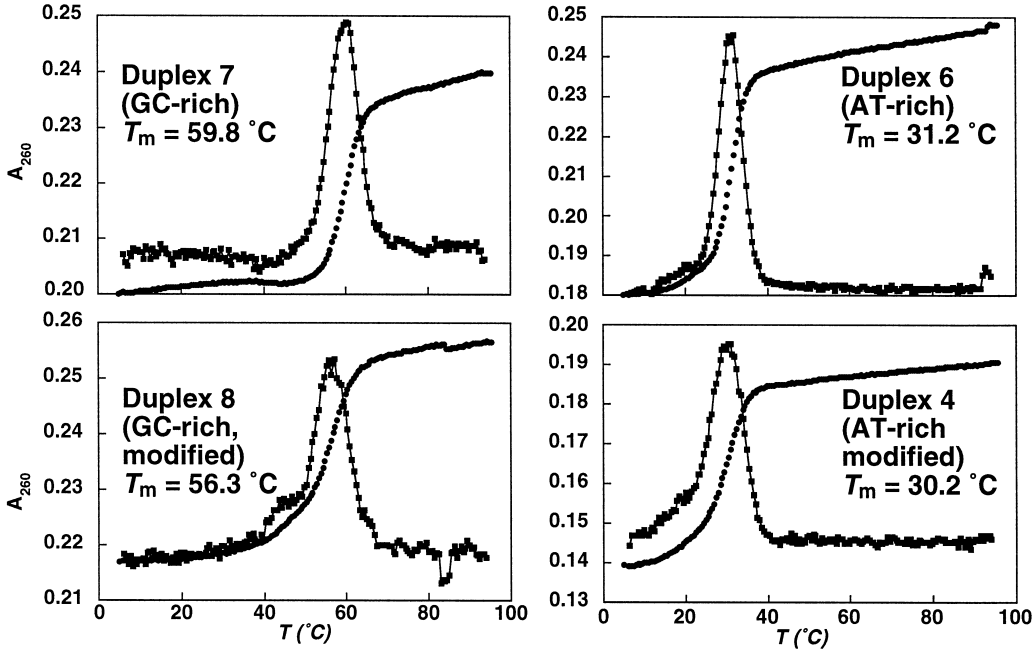

Fig. 6. The effect of methylphosphonate substitution on T_m. The indicated DNA duplexes were diluted to 5×10^{-7} M and thermal denaturation transitions were recorded as described in Section 2. (■) Absolute absorbance. (●) First derivative of the melting data.

Table 2
The effect of methylphosphonate substitution on T_m

Duplex[a]	Number of methylphosphonate substitutions	T_m (°C)[b]	Absolute difference (°C)	% T_m reduction
7	0	59.8 ± 0.2		
8	6	56.3 ± 0.1	3.6 ± 0.2	6%
6	0	31.2 ± 0.1		
4	6	30.2 ± 0.1	1.0 ± 0.2	3.2%

[a]See Fig. 1.
[b]Average ± SD based on two experiments.

tions is marginally destabilizing in both sequence contexts. The destabilization averaged 1 ± 0.2 °C for AT-rich duplexes (comparing **4** with **6**) and 3.6 + 0.2 °C for GC-rich duplexes (comparing **8** with **7**). It is unknown if and how T_m is affected by the induced DNA bending itself (apart from any destabilization due to methylphosphonate steric effects per se). We interpret these small decreases in T_m as evidence that structural perturbations due to methylphosphonate substitution are modest.

It is likely that the mixture of 2^6 stereoisomers of chiral oligonucleotides containing methylphosphonates is somewhat heterogeneous with respect to stability. This may explain the slightly broader melting transitions observed for substituted duplexes (Fig. 6). Nonetheless, the electrophoretic mobilities of ligation products on native polyacrylamide gels suggests only slight band broadening for substituted duplexes (Fig. 2). This important result demonstrates that *induced bending is a property of the entire substituted DNA population*, not just a sub-population of duplexes that contain a particularly destabilizing combination of methylphosphonate stereoisomers.

3.5. Flexibility of AT-rich DNA

The TA · AT dinucleotide within the CTAG · CTAG motif has been identified as a probable locus of anomalous torsional flexibility [19]. In crystals, this sequence shows the TA · AT dinucleotide as underwound with a twist angle of 21° [20]. It has been speculated that the increased flexibility of the TA · AT dinucleotide may represent a mechanism for facilitating alternative modes of DNA recognition and binding by proteins and for DNA positioning in nucleosomes [19].

Zhurkin et al. [11] and Olson et al. [12] have proposed a 'stochastic wedge' model to represent the inherent propensity of different bp to roll toward the major or minor grooves within dynamic DNA structures. In particular, these authors suggest that GC-rich sequences tend to be characterized by bp rolling toward the major groove (tending to widen the minor groove). In contrast, AT-rich sequences contain bp that tend to roll toward the minor groove, widening the major groove. The effects of charge neutralization along the DNA minor groove were therefore predicted to depend on how the induced electrostatic forces compressing the minor groove interact with the inherent propensity of the modified sequence to deform in that direction. According to the stochastic wedge model, GC-rich sequences should tend to resist such deformation more than AT-rich sequences. This prediction is not borne out in our data. It remains to be seen whether phosphate neutralization distributed across the major groove will show the opposite sequence dependence. Experiments to test this possibility are underway.

Our data must be contrasted with the recent results of Akiyama and Hogan [21]. These authors have studied the energetics of deforming DNA by tethering two short triple-helical regions in a manner that causes minor groove compression between them. These authors found that the electrophoretic mobility (inversely related to extent of bending) followed the relationship AT-rich > random ≥ GC-rich. The basis for this apparent resistance of AT-rich sequences to undergo minor groove compression is not understood at present.

3.6. AT-rich DNA at protein binding sites

Experiments exploring DNA bending by bZIP proteins that recognize and deform the relatively AT-rich AP-1 and/or CRE binding sites in duplex DNA have recently been reported [22–24]. All three studies involve cationic protein residues or methylphosphonate substitutions in the minor groove of DNA. In one case, neutralization of just two neighboring phosphates in the DNA minor groove was shown to eliminate intrinsic DNA bending observed within the CRE sequence [24]. These results all confirm the concept that mixed-sequence DNA will tend to respond to asymmetric phosphate neutralization by bending toward the neutralized surface. The results of the present study reinforce this point, further suggesting that such deformation is not inhibited by an AT-rich sequence context.

Numerous binding sites for DNA bending proteins are relatively AT-rich. It is interesting to note that several well-characterized protein-DNA complexes involve DNA bending toward the minor groove centered on AT-rich sequences. In the case of the *Escherichia coli* catabolite activator protein [4], the serum response factor [6], and the MATα1/MATα2 heterodimer [25], the DNA bend occurs toward the minor groove at AT-rich sequences present at the protein–DNA interface. Another intriguing example is provided by the phage φ29 protein p4 [5]. In this case, the DNA is deformed into a microloop after binding of a pair of p4 monomers. The microloop is formed by bending of an intervening AT-rich sequence toward the minor groove. These examples suggest that the ability of AT-rich sequences to accommodate minor groove bending has been exploited in nature to facilitate formation of certain nucleoprotein structures.

In some of the resulting complexes, DNA is bent in a manner consistent with collapse due to phosphate neutralization (e.g., CAP) while this is not the case for other examples (e.g., TBP). In addition to the fact that many AT-rich binding sites in duplex DNA are bent by proteins, it has also been shown that AT-rich sequences flanking protein binding sites are also important. The yeast zinc finger protein MIG1 binds to the sequence 5′-GCGGGG-3′ [26]. An AT-rich sequence 5′ to this GC box is also important for binding and is present in all natural MIG1 sites. It has been proposed that DNA binding by MIG1 could involve two steps. The zinc fingers might first bind to the GC box, followed by stabilization of the complex through bending of the DNA at the AT box allowing further protein–DNA contacts [26]. Intrinsically curved AT-rich sequences have also been shown to influence the initiation of transcription at the *E. coli* galactose operon and other bacterial promoters [27–29].

4. Conclusion

We conclude that a given degree of asymmetric phosphate neutralization about a DNA minor groove induces comparable bending in AT-rich and GC-rich contexts.

Acknowledgements

We thank D. Eicher, C. Mountjoy, and M. Doerge for oligonucleotide synthesis, and A.M. Gacy and C.T. McMurray for assistance in thermal denaturation experiments. Supported by the Mayo Foundation, NIH grants GM47814 and GM54411 to L.J.M., a University of Nebraska Medical Center Regents Fellowship to J.K.S.-S., and an NIH predoctoral training fellowship to P.D.R. Author L.J.M. is a Harold W. Siebens Research Scholar.

References

[1] G. Manning, K.K. Ebralidse, A.D. Mirzabekov, A. Rich, J. Biomol. Struct. Dyn. 6 (1989) 877.
[2] A.D. Mirzabekov, A. Rich, Proc. Natl. Acad. Sci. U.S.A. 76 (1979) 1118.
[3] J.K. Strauss, L.J. Maher, Science 266 (1994) 1829.
[4] S.C. Schultz, G.C. Shields, T.A. Steitz, Science 253 (1991) 1001.
[5] F. Rojo, A. Zaballos, M. Salas, J. Mol. Biol. 211 (1990) 713.
[6] L. Pellegrini, S. Tan, T.J. Richmond, Nature 376 (1995) 490.
[7] J.J. Love, X. Li, D.A. Case, K. Giese, R. Grosschedl, P.E. Wright, Nature 376 (1995) 791.
[8] Y. Kim, J.H. Greiger, S. Hahn, P.B. Sigler, Nature 365 (1993) 512.
[9] J.L. Kim, D.B. Nikilov, S.K. Burley, Nature 365 (1993) 520.
[10] T.K. Kerppola, T. Curran, Cell 66 (1991) 317.
[11] V.B. Zhurkin, N.B. Ulyanov, A.A. Gorin, R.L. Jernigan, Proc. Natl. Acad. Sci. U.S.A. 88 (1991) 7046.

[12] W.K. Olson, N.L. Marky, R.L. Jernigan, V.B. Zhurkin, J. Mol. Biol. 232 (1993) 530.
[13] R.I. Hogrefe, M.M. Vaghefi, M.A. Reynolds, K.M. Young, L.J. Arnold, Nucleic Acids Res. 21 (1993) 2031.
[14] D.M. Crothers, J. Drak, Methods Enzymol. 212 (1992) 46.
[15] H.-S. Koo, D.M. Crothers, Proc. Natl. Acad. Sci. U.S.A. 85 (1988) 1763.
[16] J.A. Rice, D.M. Crothers, Biochemistry 28 (1989) 4512.
[17] T.E. Haran, J.D. Kahn, D.M. Crothers, J. Mol. Biol. 244 (1994) 135.
[18] J.K. Strauss-Soukup, L.J. Maher, Biochemistry 36 (1997) 8692.
[19] M. Dlakic, R.E. Harrington, J. Biol. Chem. 270 (1995) 29945.
[20] W.N. Hunter, B.L. D'Estaintot, O. Kennard, Biochemistry 28 (1989) 2444.
[21] T. Akiyama, M.E. Hogan, Biochemistry 36 (1997) 2307.
[22] D.A. Leonard, N. Rajaram, T.K. Kerppola, Proc. Natl. Acad. Sci. U.S.A. 94 (1997) 4913.
[23] J.K. Strauss-Soukup, L.J. Maher, Biochemistry 36 (1997) 10026.
[24] D.N. Paolella, Y. Liu, A. Schepartz, Biochemistry 36 (1997) 10033.
[25] T. Li, M.R. Stark, A.D. Johnson, C. Wolberger, Science 270 (1995) 262.
[26] M. Lundin, J.O. Nehlin, H. Ronne, Mol. Cell. Biol. 14 (1994) 1979.
[27] J. Perez-Martin, M. Espinosa, J. Mol. Biol. 241 (1994) 7.
[28] M. Lavigne, M. Herbert, A. Kolb, H. Buc, J. Mol. Biol. 224 (1992) 293.
[29] F. Zuber, D. Kotlarz, S. Rimsky, H. Buc, Mol. Microbiol. 12 (1994) 231.